XANES in Nanobiology

Rebecca A. Metzler[1], Ronke M. Olabisi[1], Mike Abrecht[2], Daniel Ariosa[3], Christopher J. Johnson[4], Benjamin Gilbert[5], Bradley H. Frazer[2], Susan N. Coppersmith[1], and P.U.P.A Gilbert[1*]

[1]*Department of Physics, University of Wisconsin, Madison, WI 53706, USA*
[2]*Synchrotron Radiation Center, 3731 Schneider Drive, Stoughton, WI 53589, USA*
[3]*Institute for the Physics of Complex Matter, EPF-Lausanne, CH-1015 Switzerland*
[4]*Program in Cellular and Molecular Biology & Department of Animal Health and Biomedical Sciences, School of Veterinary Medicine, University of Wisconsin, Madison, WI 53706, USA*
[5]*Earth Science Division, Lawrence Berkeley National Laboratory, Berkeley, CA 94720, USA.*
**Previously publishing as Gelsomina De Stasio. Corresponding author: pupa@physics.wisc.edu*

Abstract. The combination of spectroscopy and microscopy enables unprecedented insights into the molecular and crystal structures of organic and inorganic materials, and their interfaces. This is relevant to the field of biomaterials in general and biominerals in particular. In this framework, we extensively analyzed various proteins, minerals and biominerals. Here we present two novel observations: x-ray absorption near-edge structure (XANES) spectroscopy at the carbon K-edge is sensitive to protein misfolding and aggregation into amyloid fibrils, and to the orientation of individual aragonite crystals in mother-of-pearl.

Keywords: XANES, X-PEEM, protein misfolding, aggregation, cross-β, nacre, orientation
PACS: 81.07.Nb, 87.15.Aa, 87.14.Ee, 87.64.Gb, 81.10.Aj

INTRODUCTION

The most sophisticated materials and machines operating on our planet are not manmade: they are produced by living organisms at the molecular, the nano-, micro- and macro-scopic scales. These "devices" not only master materials synthesis and materials performance, but they also excel at quality control and self-repair. There is a lot to learn about and from biomaterials, as we are only just beginning to understand some of the fundamental mechanisms underlying the formation of biostructures, such as templation and self-assembly. In summary, living organisms evolved to harness what we know as the laws of chemistry and physics to build the building blocks of life. They often do so with astounding efficiency: in biomineral tissues (bone, teeth, as well as the shells of crustaceans, mollusks and avian eggs, etc.), for instance, only a few percent of the mass is organic, while the rest are accurately controlled but self-assembled minerals.

The ultimate challenge for the nano-biologist is to correlate *form*, *function* and *location* of molecular structures in a cell or a tissue. Methods that can explore the chemical composition, the structure, the orientation and the position of bio-components are therefore the most desirable in the nano-biologist's toolbox. X-ray PhotoElectron Emission spectroMicroscopy (X-PEEM) combined with X-ray Absorption Near-Edge Structure (XANES) spectroscopy (= spectromicroscopy) can do all this, and more: it also reveals how different molecular structures influence one another at organic-inorganic interfaces. Furthermore, spectromicroscopy can elucidate the mechanisms of formation of biominerals, thus advancing materials science with the synthesis of novel bio-inspired materials.

Here we discuss two particular recent experiments in nanobiology, in which we revealed that XANES spectroscopy is sensitive to the specific macro-molecular structure of amyloid-forming molecules associated with diseases, and to the crystal orientation in mollusk shells. Interestingly, in both cases, unexpected spectroscopic results were first observed in the bio-system, then fully studied, characterized and explained in model, abiotic samples, then the spectroscopic interpretation was used to go back to the biosystem and produce biologically relevant results.

CP882, *X-ray Absorption Fine Structure—XAFS13*
edited by B. Hedman and P. Pianetta

XANES Detects Protein Misfolding and Aggregation

We examined the ability of carbon K-edge XANES spectroscopy to detect protein and polypeptide conformation. Figure 1 shows spectra collected from poly-L-Lysine (PLL), a synthetic homopolypeptide that can be folded into α-helical or β-pleated sheet conformations but also forms cross-β fibrils [1, 2], the molecular assembly commonly called amyloid, which is common to other naturally misfolded and aggregated proteins, associated with Alzheimer's, Parkinson's, and Mad Cow diseases [3]. In cross-β fibrils, β strands run perpendicular to the fibril axis [1, 2, 4-9].

Spectra of α-PLL and β-PLL are shown in Figure 1A and represent the non-fibril forming conformations of PLL. These spectra are almost indistinguishable, indicating that, at least in PLL, carbon K-edge XANES spectroscopy cannot distinguish between α and β conformations. In Figure 1B we present XANES spectra collected from α-PLL and cross-β-PLL (PLL samples kept, respectively, for 0 and 2 days at pH 11.1 and 65°C). The comparison of these two spectra demonstrates that carbon K-edge XANES spectroscopy can clearly distinguish cross-β fibrils. The most significant difference is the enhancement of peak 2 at 287 eV, "the amyloid peak", and a shift in energy of peak 3 at ~288 eV. Peak fitting enables the quantification of spectral features and was applied to all spectra in Figure 1. Interestingly, the single Lys spectrum does not significantly differ from the PLL spectrum, in which 1,000-2,000 Lys residues are present. This simplified peak assignment, which is as follows: peak 1 at 285 eV, corresponds to the C1s→π* transition in C=C double bonds; peak 2 at 287 eV is the C-H C1s→σ*, mostly due to PLL side chains; peaks 3 and 4 at ~288 eV are both associated with C=O C1s→π*; peak 5 at ~290 eV, corresponds to the C1s→π* transition in C=O double bonds in carbonates [10, 11].

To ensure that the spectral differences observed in Figure 1B are due to cross-β fibril formation and not to other chemical or physical effects, we conducted extensive and systematic radiation damage studies on PLL. These revealed that while peaks 1 and 5 are radiation-damage induced, peak 2 is not. Carbonates in particular (peak 5), accumulate due to the harsh chemical conditions necessary to form cross-β-PLL and prolonged storage or under increasing exposure to 288.2 eV radiation, but have nothing to do with the presence or absence of fibrils. We conclude that the peak 2 enhancement and peak 3 energy shift observed in Figure 1B cannot be radiation damage induced.

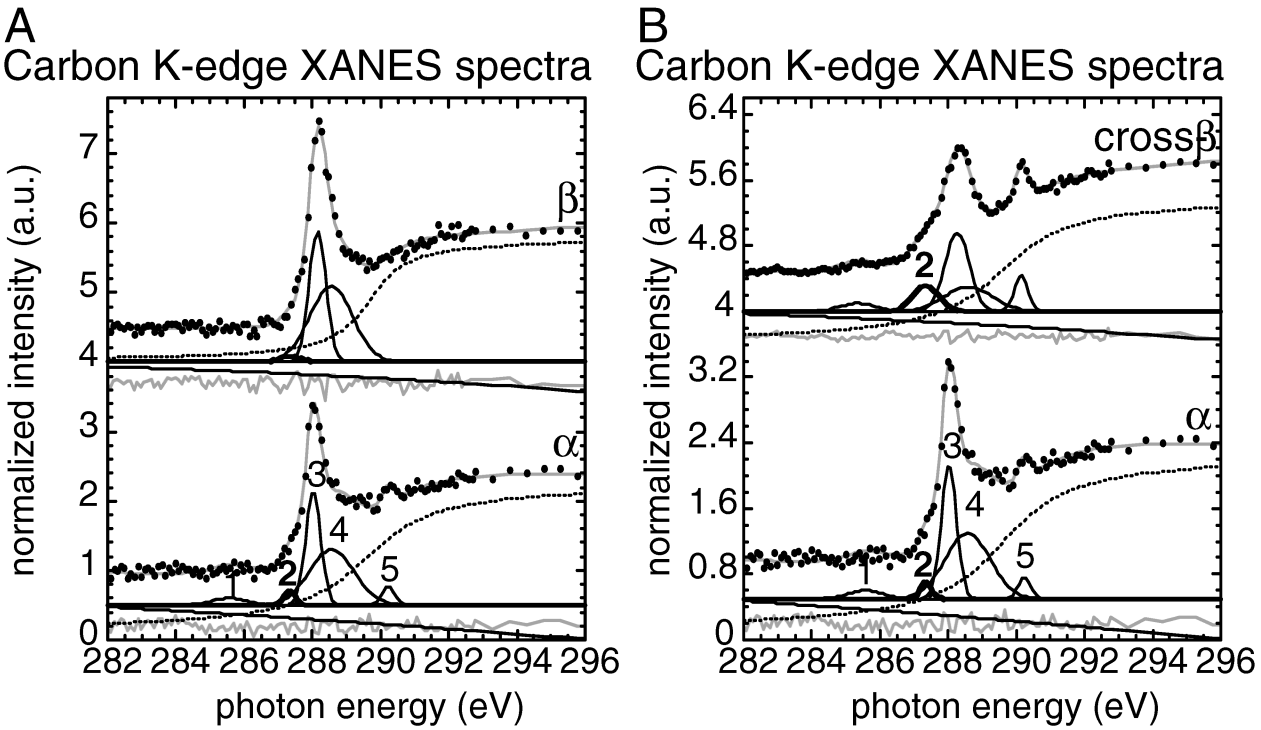

FIGURE 1. (**A**) Carbon K-edge XANES spectra for α-PLL (day 0 at pH 11.1) and β-PLL (day 4 at pH 11.1 and 65°C, supernatant) show that XANES spectroscopy cannot determine protein folding. (**B**) Carbon K-edge XANES spectra from α-PLL and cross-β-PLL shows that XANES spectroscopy detects the cross-β fibril through the enhancement of peak 2, "the amyloid peak".

After discovering the sensitivity of XANES to the cross-β structure in synthetic PLL, we extended the study to more relevant, and more complex natural proteins, which also form the cross-β structure. These include β-amyloid peptide (Aβ, residues 1-40), prion protein extracted from scrapie-infected (PrP^{Sc}) and uninfected hamster brains (PrP^{C}), and the Sup35 yeast prion's amyloid-forming nucleus, containing only 7 amino acids: GNNQQNY [4, 5]. In all systems examined, peak 2 enhancement occurred in the cross-β form of the protein. Additional radiation damage studies on Aβ confirm that peak 2 is independent of radiation dose and therefore can be confidently assigned to fibril formation.

XANES Detects Orientational Disorder in Nacre Crystalline Tablets

We examined *Haliotis rufescens* (red abalone) using a combination of X-PEEM and XANES spectroscopy. In doing so, we imaged and extracted XANES spectra from individual nacre (mother-of-pearl) and prismatic tablets using the Spectromicrsocope for PHotoelectron Imaging of Nanostructures with X-rays (SPHINX) [12, 13, 14].

In Figure 2 we present calcium, oxygen, and additional useful method to examine protein misfolding and aggregation.

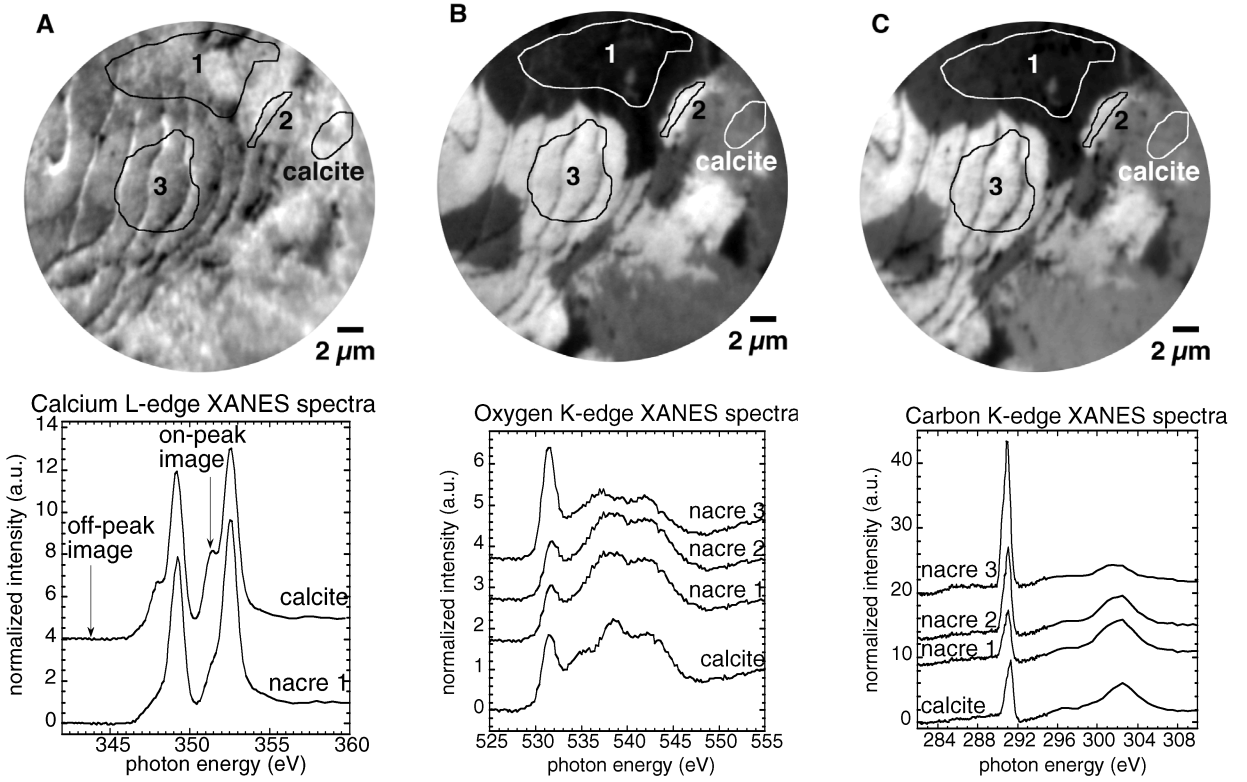

FIGURE 2. (**A**) Calcium distribution map of the polished surface of red abalone at the boundary between the outer shell prismatic layer (calcite) and the inner nacre layer (aragonite). The Ca map was obtained by digital ratio of two X-PEEM images acquired with SPHINX, on- and off-peak. The on-peak was acquired at 351.3 eV, on the crystal field peak, which is strong in calcite and weak in aragonite. Below the distribution map are the XANES spectra extracted from a representative nacre tablet (all Ca spectra from different nacre tablets are alike), and a prismatic column, showing that calcite is on the right of the border and aragonite on the left. (**B, C**) Distribution maps of the same region as seen in (**A**) for the oxygen and carbon π* signals obtained by digital ratio of images at 531.5 eV and 516 eV, and 290.2 eV and 278 eV, respectively. Below the oxygen and carbon maps are XANES spectra extracted from the correspondingly labeled regions within the maps, showing that the tablets in the nacre region have strongly varying intensities of the π* peak.

These results demonstrate for the first time the ability of XANES to distinguish between normally folded proteins and misfolded proteins aggregated into cross-β fibrils. XANES spectroscopy is, therefore, an

carbon distribution maps obtained by imaging the polished surface of red abalone. Figure 2A shows with different grey levels the enhancement (darker grey) of the crystal field peak at 351.3 eV, which is more

prominent in the calcium L-edge XANES spectrum of calcite and than in aragonite [15]. Despite the poor energy resolution of the calcium spectra extracted from this region, it is possible to identify the imaged region as the nacre-prismatic boundary in the shell, with nacre (aragonite) on the left and the outer prismatic shell layer (calcite) on the right. In Figure 2B and 2C we present, respectively, the oxygen and carbon distribution maps in which the different grey levels indicate the intensity of the π* peak (531.5 eV for the O1s→π* transition of the C=O double bond and 290.2 eV for the C1s→π* transition of the C=O double bond) [16, 17].

The intensity of the π* peak depends on the crystallographic orientation of each nacre or prismatic tablet with respect to the linearly polarized light from the synchrotron. In Figure 2B and Figure 2C, notice how immediately adjacent tablets in the nacre region have completely different grey levels (π* peak intensity). Additionally, we found that the tablet contrast observed near the nacre-prismatic boundary continued several hundreds of microns into the nacreous region.

Immediately below Figures 2B and 2C are XANES spectra taken at the oxygen and carbon K-edges, respectively, from correspondingly labeled tablets of Figures 2B and 2C. These spectra quantify the π* peak intensity difference observed in the distribution maps and led us to investigate the polarization-dependence of XANES spectroscopy of carbonates.

The contrast in Figures 2B and 2C is due to crystallographic orientation disorder in nacre tablets. Specifically, the directions of the *c* axes of different nacre tablets differ, consequently the polar angle, that is, the angle between the *c* axis and the polarization vector varies from tablet to tablet. The observed variation could, therefore, be described as polar angle disorder.

We produced theoretical XANES spectra using FEFF 8.2 [17, 18, 19]. The simulated spectra exhibit a strong dependence of the π* peak intensity on polar orientation. To conclusively assign the source of contrast to polar rotation, however, we collected carbon K-edge XANES spectra from natural aragonite crystals. Spectra were obtained for polar rotation angles varying between 0° and 90°, and found to show dramatically different π* intensities. Although a quantitative assignment of nacre tablet orientation angles is not yet possible, the results on aragonite confirm that the contrast observed in nacre is due to polar disorder.

The strong crystal orientation dependence of carbon K-edge XANES spectra enabled us to map individual tablets, or stacks of tablets, in red abalone due to disorder in tablet orientation. Further investigation into this contrast-generating mechanism is necessary for quantitative results. For the moment, its discovery led to new insights into the nacre formation mechanism, which has been and remains elusive.

ACKNOWLEDGMENTS

Funding for this work was provided by grants: NSF-PHY-0523905, UW-135-A018-A-48-6700, UW-135-F054-A34-4867, and AFOSOR-FA9550-05-1-0204 to PUPAG, NSF-DMR-0209630 to SNC. The experiments were carried out at the UW-Synchrotron Radiation Center, supported by NSF-DMR-0084402.

REFERENCES

1. Fandrich, M. & Dobson, C. M. The behaviour of polyamino acids reveals an inverse side chain effect in amyloid structure formation. *EMBO J.* **21**, 5682-5690 (2002).
2. Petkova, A. T. *et al*. A structural model for Alzheimer's beta -amyloid fibrils based on experimental constraints from solid state NMR. *Proc. Natl. Acad. Sci. U. S. A.* **99**, 16742-16747 (2002).
3. Nelson, R. & Eisenberg, D. Recent atomic models of amyloid fibril structure. *Current Opinion in Structural Biology* **16**, 260-265 (2006).
4. Balbirnie, M., Grothe, R., Eiseberg, D. S. *Poc Natl Acad Sci* **98**, 2375-2380 (2001).
5. Nelson, R. *et al*. *Nature* **435**, 773-778 (2005).
6. Govaerts, C., Wille, H., Prusiner, S. B. & Cohen, F. E. Evidence for assembly of prions with left-handed beta-helices into trimers. *Proc. Natl. Acad. Sci. U. S. A.* **101**, 8342-8347 (2004).
7. Sunde, M. *et al*. Common core structure of amyloid fibrils by synchrotron X-ray diffraction. *J. Mol. Biol.* **273**, 729-739 (1997).
8. Perutz, M. F., Finch, J. T., Berriman, J. & Lesk, A. Amyloid fibers are water-filled nanotubes. *Proc. Natl. Acad. Sci. U. S. A.* **99**, 5591-5595 (2002).
9. Diaz-Avalos, R. *et al*. *J Mol Biol* **330**, 1165-1175 (2003).
10. Myneni, S. C. B. in *Reviews in Mineralogy and Geochemistry: Applications of Synchrotron Radiation in Low-Temperature Geochemistry and Environmental Sciences* (eds Fenter, P., Rivers, M., Sturchio, N. & Sutton, S.) 485-579 (Mineralogical Society of America, Washington, DC, 2002).
11. Kaznacheyev, K. *et al*. Innershell absorption Spectroscopy of amino acids. *J. Phys. Chem. A* **106**, 3153-3168 (2002).
12. Gilbert, P.U.P.A., Frazer, B.H., Abrecht, M. In: *Molecular Geomicrobiology*. (vol. 59 Mineralogical Society of America, Washington DC, 2005) p. 157-185, JF Banfield, KH Nealson, J. Cervini-Silva (eds).
13. Frazer, B.H., Girasole, M., Wiese, L.M., Franz, T., De Stasio, G. Spectromicroscope for the Photoelectron Imaging of Nanostructures with X-rays (SPHINX):

performance in biology, medicine and geology. *Ultramicroscopy* **99**, 87-94 (2004).
14. De Stasio, G., Frazer, B. H., Gilbert, B., Richter, K. L., Valley, J. W. Compensation of charging in X-PEEM: a successful test on mineral inclusions in 4.4 Ga old zircon. *Ultramicroscopy* **98**, 57 (2003).
15. Gilbert, P.U.P.A., Frazer, B.H., Abrecht, M. In: *Molecular Geomicrobiology*. (vol. 59 Mineralogical Society of America, Washington DC, 2005) p. 157-185, JF Banfield, KH Nealson, J. Cervini-Silva (eds).
16. Madix, R.J., Solomon, J.L., Stohr, J. The orientation of the carbonate anion on Ag(110). *Surface Science* **197**, L253 (1988).
17. Stohr, J. *NEXAFS Spectroscopy* (Springer-Verlag, Berlin, 1992).
18. Ankudinov, A.L., Bouldin, C., Rehr, J.J., Sims, J., Hung, H. Parallel calculation of electron multiple scattering using Lanczos algorithms. *Phys. Rev. B.* **65**, 104107 (2002).
19. Wise, S.W. Microarchitecture and mode of formation of nacre (mother-of-pearl) in pelecypods, gastropods, and cephalopods. *Eclogae Geol. Helv.* **63**, 775-797 (1970).
20. Caspi, E.N., Pokroy, B., Lee, P.L., Quintana, J.P., Zolotoyabkob, E. On the structure of aragonite. *Acta Cryst.* **B61**, 129 (2005).